Research article

Nanoindentation simulation of concrete with various indenter forms and yield strengths

Nasser Asroun, Aissa Asroun
Civil Engineering and Environment Laboratory, Djillali Liabes University
PO box 89 Sidi Bel-Abbes 22000 Algeria
a_asroun@yahoo.fr

ABSTRACT

In present work, the finite element method was used to simulate the whole process of nanoindentation test. Two kinds of indenters, spherical and conical, were used to simulate indentation test of concrete. The modeling procedures were introduced in detail. The agreement between the FE calculations and experimental results is satisfactory with appropriate geometry parameters and mechanical properties of specimen materials. The indenter tip shape and the yield strength of concrete have significant effect on the accuracy of simulation results.

Keywords: Simulation, concrete, indenter, yield strength, nanoindentation.

1. Introduction

Indenters are usually made of diamond. These indenters are very hard, but are also very brittle and can be broken easily. The mechanical properties of diamond vary due to the crystalline nature of the diamond structure. Values for modulus range from about 800 GPa to 1200 GPa in literature. A value of 1141 GPa is usually used in the analysis of nanoindentation test data with a Poisson's ratio of 0.07 (Fischer-Cripps, 2004). The aim of the nanoindentation tests is to obtain the elastic modulus, hardness and deformation of the specimen material through load-displacement measurements. The depth of penetration beneath the specimen surface is measured as the load is applied to the indenter. Therefore, the size of contact area can be determined by the known geometry of the indenter. There are several types of indenters used in nanoindentation testing. Indenters can be classified into two categories: sharp or blunt. Generally speaking pyramidal and conical indenters are sharp and spherical indenters can be considered as blunt. The Berkovich indenter is generally used in small scale indentation testing (Berkovich, 1951). It has the advantage that edges of the three-sided pyramid are more easily constructed to meet at a single point compared to those edges of the four-sided Vickers pyramid. The face angle of the Berkovich indenter normally used in nanoindentation testing is 65.27 degrees. The tip radius for a new Berkovich indenter is about 50-100 nm, which usually increases to about 200 nm with use (Fischer-Cripps, 2004). Conical indenters have the advantage of axial symmetry. For a Berkovich indenter, the equivalent conical indenter has a semi-angle of 70.3 degrees (Lichinchi et al. 1998). When analyzing nanoindentation test data taken with Berkovich indenters, it is convenient to use an equivalent axial-symmetric conical indenter for simplification (Lichinchi et al. 1998). Spherical indenters are especially suitable for testing soft materials. This type of indenters provides a smooth transition from elastic to elastic-plastic contact (Walter et al. 2007).

2. Analysis methods

2.1 Berkovich indentation analysis

The load-indentation data for samples indented with the Berkovich indenter was analyzed using the method outlined by Oliver and Pharr (1992). In this method, properties of indented material were derived from the unloading portion of the load-depth curve gathered during the nanoindentation experiment. This method's major parameters are shown in Figure 1.

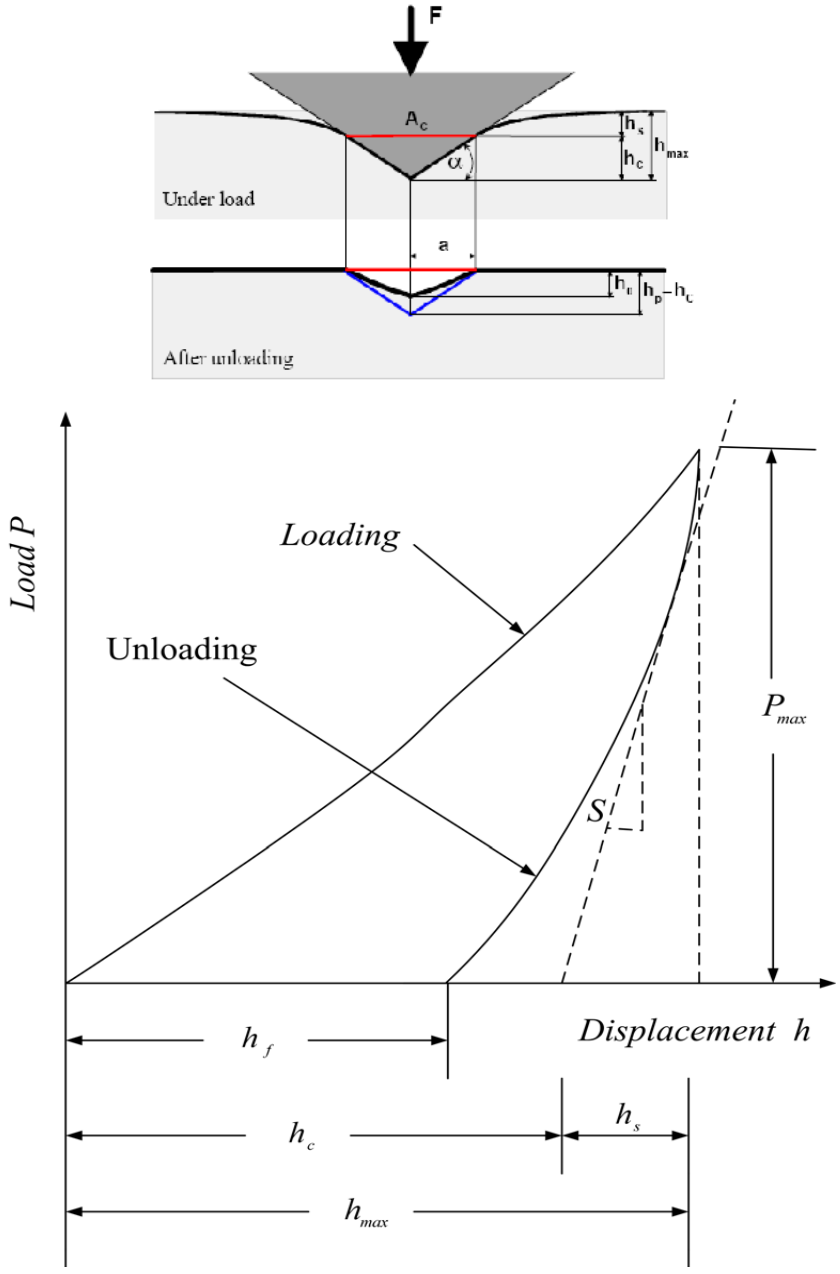

Figure 1: Parameters of the oliver and pharr methods

The total indentation depth h_{max} is defined as the sum of h_c and h_s

$$h_{max} = h_c + h_s \quad (1)$$

h_c: indenter contact depth

h_s: displacement at the surface at the perimeter of the indentation

The contact area is then determined by relating the cross-sectional area to h_c. Typically the contact area for a Berkovich indenter *A* is given as

$$A = 24.5h_c^2 \quad (2)$$

h_c: indenter contact depth ($h_{max} - h_s$ from Equation (1))

Once the contact area is computed, the hardness of the specimen can then be computed. The hardness is defined as the ratio of P_{max} to *A*.

$$H = \frac{P_{max}}{24.5h_c} \quad (3)$$

P_{max} : maximum indentation load.

Nanoindentation also allows equating the contact stiffness of the indented material to Young's modulus of elasticity. Here the term "reduced modulus" is used in place of Young's modulus to account for the affect of the indenter stiffness on measurements. The reduced modulus E_r can be derived from Equation (4).

$$\frac{1}{E_r} = \frac{1-\nu^2}{E} + \frac{1-\nu'^2}{E'} \quad (4)$$

ν : Poisson's ratio of the indented material
E : Young's modulus of the indented material
ν': Poisson's ratio of the indenter (0.07)
E': Young's modulus of the indenter (1141 GPa).

Considering the above relations, E_r can be defined as

$$E_r = \frac{\sqrt{\pi}}{2}\frac{1}{\beta}\left(\frac{S}{\sqrt{24.5h_c^2}}\right) \quad (5)$$

β : correction factor (1.034 for the Berkovich indenter (Fischer-Cripps, 2004))

S : contact stiffness

Determining the contact stiffness (*S*) requires curve fitting of the loading and unloading curves using a power law function. For the unloading portion of the curve the relation can be represented as

$$P = \omega(h - h_r)^2 \quad (6)$$

ω: a curve fitting constant

h : indentation depth

h_r : residual indentation depth.

Expanding this equation gives a quadratic equation with three constants *A*, *B*, and C shown in equation (7).

$$P = A(h)^2 + B(h) + C \quad (7)$$

A, *B*, and *C:* coefficients determined by fitting the equation to the top 60% of the unloading curve. Then the slope of the unloading curve (*S*) can be computed as the gradient of the power function at maximum depth.

$$S = \frac{dP}{dh} = 2A(h_{max}) + B \quad (8)$$

A and *B* : coefficients determined by fitting the equation to the unloading curve

h_{max}: maximum indentation depth.

2.2 Spherical indentation analysis

For analysis of the nanoindentation data gathered from using the spherical indenter, the Oliver and Pharr method was applied to the spherical indenter (Fischer-Cripps, 2004). This method recognizes the variation of the indented radius with depth. Figure 2 shows the major variables used in this analysis.

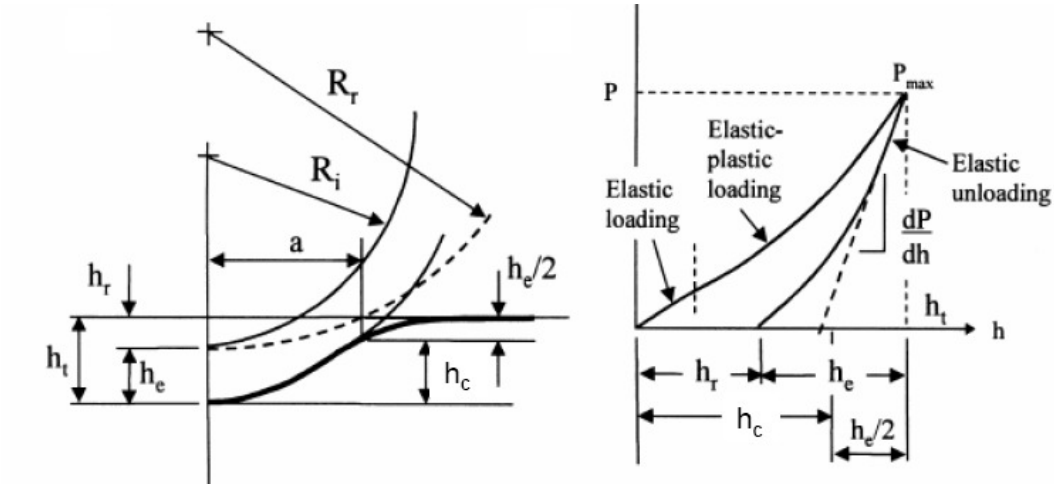

Figure 2: Schematic of parameters for spherical indenter

The total indentation depth h_t is the sum of the plastic depth and the half of the elastic displacement, shown in Equation (9).

$$h_t = h_p + \frac{h_e}{2} \quad (9)$$

h_p: plastic indentation depth

h_e: elastic displacement

The elastic displacement h_e is defined in Equation (10) (Hertz, 1881).

$$h_e = \frac{a^2}{R} \quad (10)$$

a: radius of the circle of contact at maximum load.

R : relative radius of curvature of the residual impression; where a can be calculated as a function of the plastic depth and the indenter radius as described by Equation (11).

$$a = \sqrt{2R_i h_p - h_p^2} \quad (11)$$

R_i : indenter radius (25 µm for this work)

The relative radius of curvature R is defined as

$$\frac{1}{R} = \frac{1}{R_i} - \frac{1}{R_r} \tag{12}$$

R_i : indenter radius

R_r : radius of curvature of the residual impression.

The contact area A can be calculated from the radius of the circle of contact a. As mentioned earlier, Oliver and Pharr (1992) recognized that the unloading curve for a majority of materials indented followed a power fit rather than a strict linear relationship. They noted these phenomena for a Berkovich indenter, but this method can be applied to other indenters. For this work, a power function was fit to top 60% of the unloading curve and the slope of indentation load-depth curve (dP/dh) was calculated as the slope of a line tangent to the power fit relationship or the derivative of the power fit relationship, as described in the Berkovich analysis. Once the contact area and slope were determined, the reduced modulus E_r can be calculated as

$$E_r = \frac{dP}{dh}\frac{1}{2a} = \frac{1}{2}\frac{dP}{dh}\frac{\sqrt{\pi}}{\sqrt{A}} \tag{13}$$

A : contact area

a : radius of the circle of contact at maximum load.

3. Finite element modeling

The model consists of the simulation of nanoindentation test of concrete on 2D planar model using the commercial finite element package ANSYS v.11.0 (2011). Both Berkovich and spherical diamond indenter were used to perform the indentation process in this work. The first had a pyramid shape with face angle of 65.27°. It has commonly modeled as a conical indenter with a semi-apex angle of 70.3 degrees. The second had a spherical shape with a 50 µm of diameter. A square area with dimensions including a base of 600 µm, a height of 600 µm was created to represent the concrete specimens. The indenter and specimen are meshed by 2D structural PLANE182 element as shown in Figure 3.

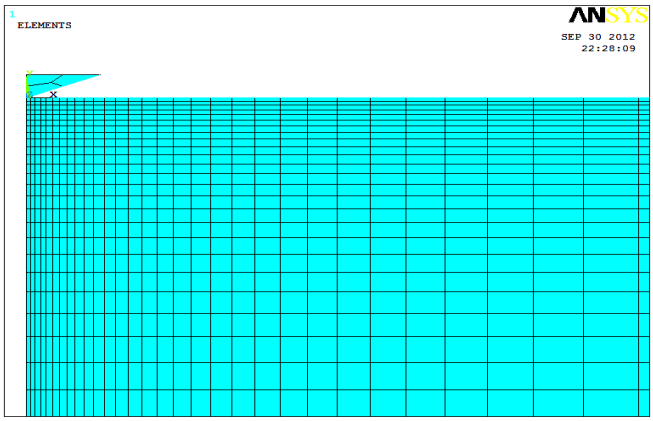

Figure 3: FE model of indenter and concrete specimens

Nodes along the centerline are constrained to move in x-direction and the nodes at the bottom line are constrained to move in x and y-directions. Axisymmetry conditions are applied along the centerline. The interaction of the indenter and the specimen is modeled as a contact pair with no friction. Contact element TARGET169 is applied to the Berkovich or spherical

indenter and CONTACT172 to the specimen. The specimens were subjected to a trapezoidal Load history with varying magnitude of peak indentation load. The loading, dwelling and unloading periods were kept at varying times and were applied to the upper portion of the indenter in *y*-direction. The displacement in *y*-direction along the upper line of the specimen is measured.

For the diamond indenter an elastic linear isotropic model with Young modulus $E_i = 1141\ GPa$ and Poisson ratio $\nu_i = 0.07$ was used. Young's modulus, hardness, Poisson's ratio of different concretes and time of loading was presented in Table1.

Table 1: Material properties of indented concretes

Material	E (GPa)	H (GPa)	ν	Time of load	Indenter type
NVC30(Reinhardt, 2010)	45	0.26	0.25	10-180-10 (P_{max}=0.5mN)	Berkovich
NVC30(Reinhardt, 2010)	45	0.23	0.25	20-180-20 (P_{max}=1mN)	Berkovich
SCC17(Prasad, 2012)	16	0.033	0.25	20-120-20 (P_{max}=0.5mN)	Spherical
UHPC165(Ahlborn,2011)	54.1	0.461	0.21	20-120-20 (P_{max}=0.5mN)	Spherical
HS of OPC*(Kaushal, 2012)	38.95	1.21 ± 0.35	0.25	10-2-10 (P_{max}=0.5mN)	Berkovich

*: High Stiffness forms of C-S-H phase of Ordinary Portland Cement.

The distribution curves of indentation depth over load for low strength concrete (SCC17), Ultra high strength concrete (UHPC165) indented with Berkovich indenter and normal strength concrete (NVC30) indented with spherical indenter were dressed and compared with experimental ones.

4. Results and discussions

4.1 Effect of indenter shape on simulation results

In this study, both the Berkovich and spherical indenters produced meaningful results from different concretes. Figure 4 shows the load-displacement curves obtained by Berkovich and spherical indenters. In Figure 4.a, Berkovich indenters produces large amount of numerical indentation depth compared with experimental ones for NVC30 concrete both for 0.5mN and 1mN. In the figure 4.b, the spherical indenter produces approximativelly the same amount of indentation depth for SCC17 and UHPC165 between the numerical and experimental curves. These results are explained by the sharpness of the Berkovich indenter which it penetrates into concrete sample more than a spherical indenter under the same amount of load.

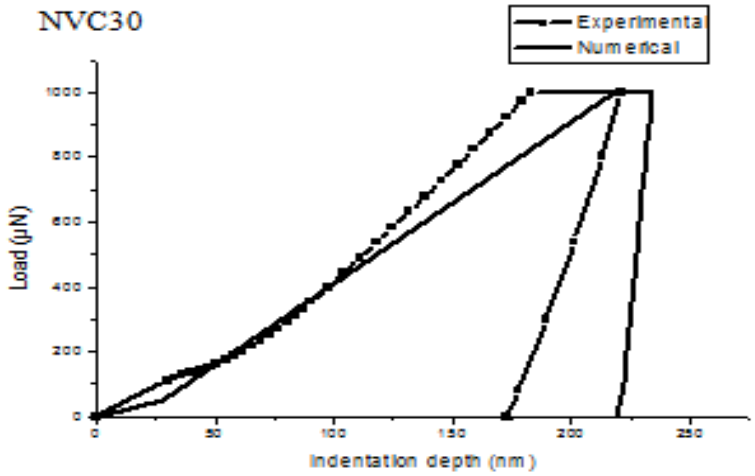

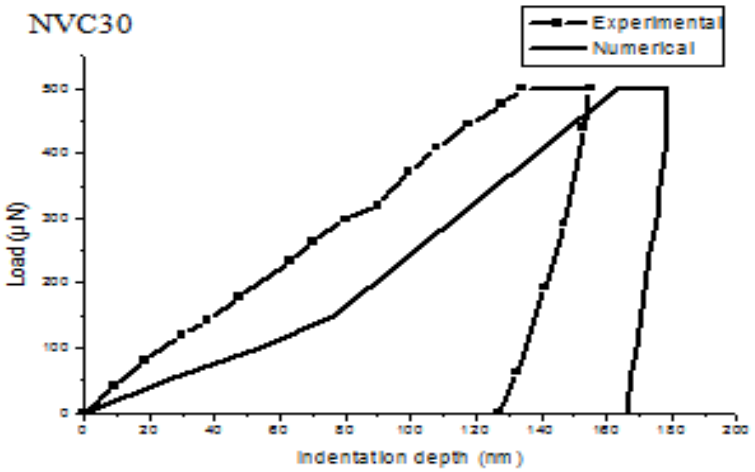

a) Berkovich indenter

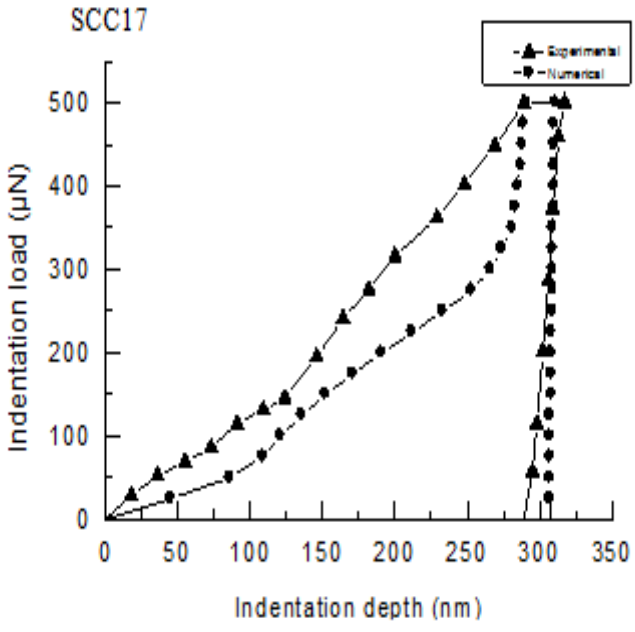

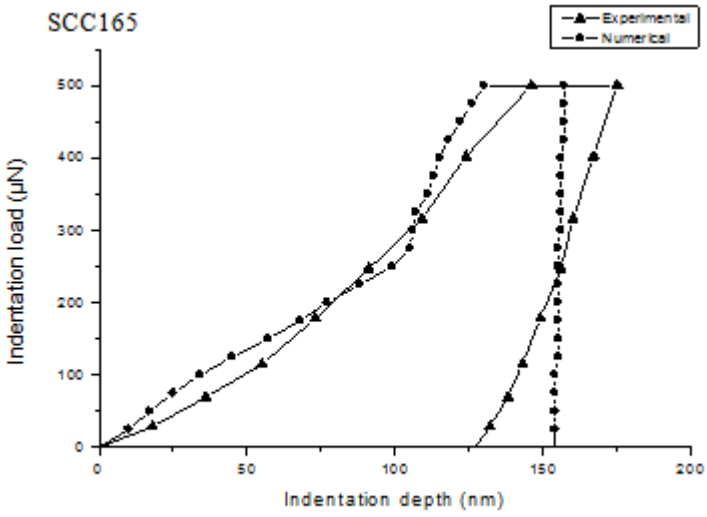

b) spherical indenter

Figure 4: Indentation curves of different concretes with a) Berkovich and b) spherical indenter

4.2 Effect of concrete yield strength on simulation results

However, thorough discussion of the effect of materials mechanical properties on nanoindentation simulation is rare. Usually, the material properties used in numerical simulation are simplified. In previous section, the material property of concrete is assumed to be elastic-perfectly plastic with the yield strength of 403 MPa. However, the actual stress and strain relationship of this material is more complicated. Besides, yield strength of concrete can be much higher or much lower. This factor can affect the accuracy of numerical results.

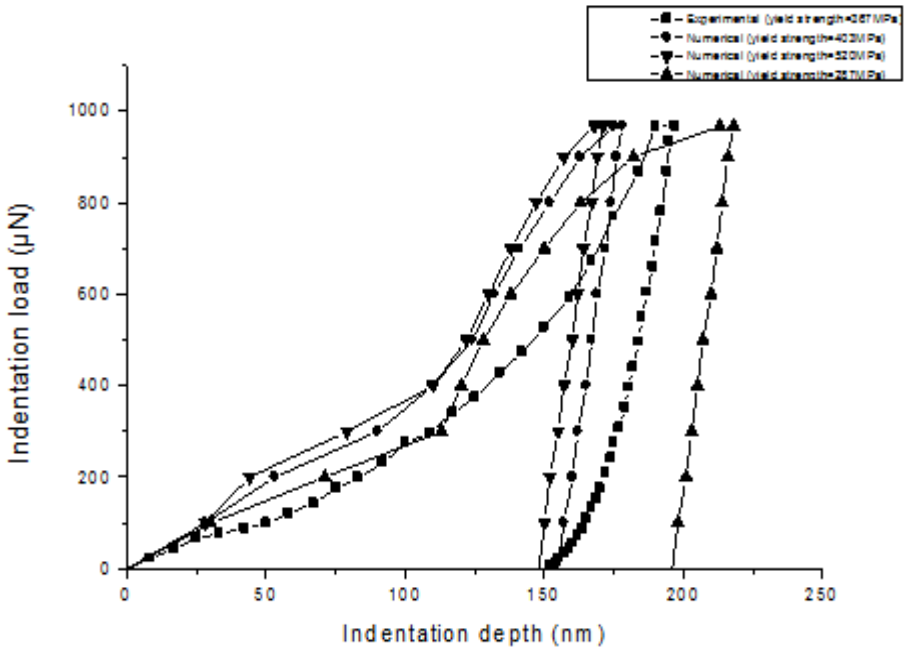

Figure 5: Indentation curves with varying yield strength of High Stiffness forms of C-S-H phase of OPC

Figure 5 shows the effect of concrete yield strength on simulation results in our model. With increasing yield strength of the concrete, the maximum indentation depth of numerical results decreases, and the loading, holding and unloading parts of the curve can get closer to experimental data. The bulk concrete yield strength of 287 MPa is too small to be realistic in this simulation. When the value of yield strength changed from 520 MPa to 403 MPa, the maximum indentation depth increased by 4%. The numerical results demonstrated smaller sensitivity to the change of concrete yield strength in this model than the change of tip shape in the previous section. A perfect fit can be obtained given the appropriate yield strength value and the indenter shape.

5. Conclusion

According to the analysis of the data obtained from nanoindentation simulation of concrete under different indenter forms and yield strengths, we can conclude that

1. The FE model has been developed to simulate the indentation process of different concrete strength. The model is capable of simulating the loading-holding-unloading stages with two indenter shape Berkovich and spherical. The indentation depths of the Berkovich indenter were larger than the spherical ones for different concrete strength and different maximum load.
2. The sensitivity of our numerical results to the change of concrete yield strength was less than the change of tip shape of indenter with a percent of 4%.
3. The agreement between the FE calculations and experimental results is satisfactory with appropriate geometry of indenter and appropriate yield strength of concrete specimens.

Acknowledgement

This work was supported in part by the National Council of Evolution of University Projects of Research of Algeria under Grant number CNEPRU J0402120090080.

6. References

1. Ahlborn.T.M, Harris D.K, Misson D.L and Peuse E.J, (2011), Strength and durability characterization of ultra-high performance concrete under variable curing conditions, Transportation research board annual meeting, 22(51), pp 68-75.

2. ANSYS v.11.0, (2011), user manual ANSYS Inc. 2007.

3. Berkovich E.S., (1951), Three-faceted diamond pyramid for micro-hardness testing. Indian Diamond Revue, 11(127), pp 129-133.

4. Fischer-Cripps A.C., (2004), Nanoindentation, Second edition, New York Springer, 260.

5. Kaushal K. Jha, Nakin Suksawang, Debrupa Lahiri and Arvind Agarwal., (2012), American Concrete Institute materials journal, 109(1), pp 81-90.

6. Lichinchi M., Lenardi C., Haupt J. and Vitali R., (1998), Simulation of Berkovich nanoindentation experiments on thin films using finite element method, Thin solid films, 312(1-2), p 240.

7. Oliver W.C. and Pharr G.M., (1992), An improved technique for determining hardness and elastic modulus using load and displacement sensing indentation experiments, Journal of Materials Research, 7(4), pp 1564-1583.

8. Prasad R.V.R.K., (2012), Experimental investigation of Use of Microsilica in Self Compacting Concrete, Indian streams research journal, 2(4), pp 1-4.

9. Walter C., Antretter T., Daniel R. and Mitterer C., (2007), Finite element simulation of the effect of surface roughness on nanoindentation of thin films with spherical indenters, Surface and coatings technology, 202(4-7), p 1103.